THEORETICAL ANALYSIS OF THE RADIATION FIELDS OF A SHORT BACKFIRE ANTENNA FED BY A RECTANGULAR WAVEGUIDE

Z. A. AHMED*
A. A. OBAID**

SUMMARY: Mathematical expressions in closed form for the radiation fields of the short backfire antenna have been derived, based upon the current distribution method. The calculated patterns are found to be in good agreement with the measured patterns given by other research workers.

Key Words: Radiation fields, backfire antenna.

INTRODUCTION

The backfire antenna was originally described in 1960 by H.W. Ehrenspeck (1) and a much simplified version called the short backfire antenna was introduced by the same author in 1965 (2). Since then the short backfire antenna has been the subject of extensive experimental studies (3-10). However, only a few papers have theoretically investigated this structure (11-13). It is the purpose of this paper to report theoretical analysis for the radiation fields of the short backfire antenna shown in Figure 1.

SBFA consists of two parallel circular metal plates of unequal diameters. These were placed perpendicular and co-axial to the central axis of the antenna and were spaced by a half wavelength. A rectangular smooth walls waveguide, used as a feeder to excite the antenna with a microwave energy, was positioned midway between and parallel to the plates. The front small plate which is called sub-reflector acts as a mirror to reflect the wave incident from the excitor back toward the large plate called main-reflector which in turn reflects the wave back again to an observation point located in the front of the antenna as shown in Figure 2.

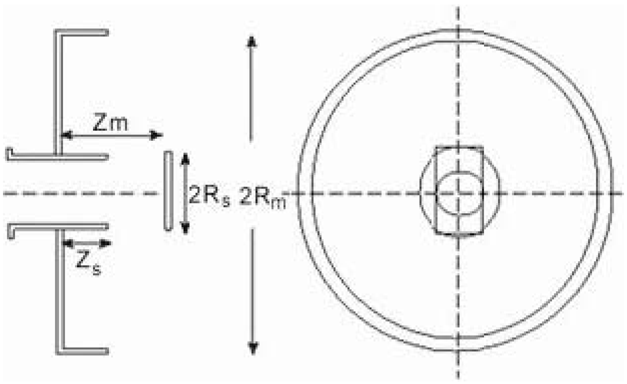

Figure 1: Sketch of SBFA.

*From Department of Physics, College of Science, University of Basrah, Basrah, Iraq.
**From Department of Physics, College of Education, University of Basrah, Basrah, Iraq.

Analysis of the radiation fields:

The analysis begins by considering a rectangular waveguide of dimensions a and b in x and operating and y direction, respectively, centered on the origin, and operating in the dominant TE_{10} mode, which has a cosine distribution in the broad dimension and a uniform distribution in the narrow dimension. The tangential fields in the aperture of the excitor are:

$$\underline{E}_a = \hat{y}E_{ya} = \hat{y}E_o \cos\left(\frac{\pi}{a}x\right) \text{ ....(1-a)}$$

$$\underline{H}_a = \hat{y}H_{xa} = \hat{x}(-E_{ya} / Zg) \text{ ....(1-b)}$$

where $Zg = \omega\mu / \beta$ is the waveguide impedance for TE waves, and β is the wave number corresponding to the free space wavelength. The radiation field of the excitor at an observation point P (r_1, $\varnothing_1$, θ_1) may be calculated by a well-known technique (14) based on the equivalent electric and magnetic surface current densities, where only transverse θ and $\varnothing$ components are retained, as:

$$\underline{E}_1 = j\boldsymbol{\beta}\frac{e^{-j\beta r_1}}{4\pi r_1}(1+\cos\boldsymbol{\theta}_1)P_y(\hat{\boldsymbol{\theta}}\sin\varnothing_1 + \hat{\varnothing}\cos\varnothing_1) \text{ ..... (2-a)}$$

$$\underline{H}_1 = \frac{1}{Z_0}\hat{r}\times\underline{E}_1 = -j\boldsymbol{\omega\varepsilon}\frac{e^{-j\beta r_1}}{4\pi r_1}(1+\cos\boldsymbol{\theta}_1)Py(\hat{\boldsymbol{\theta}}\cos\varnothing_1 - \hat{\varnothing}\sin\varnothing_1) \text{ ......(2-b)}$$

where:

$$P_y = \int_s E_{ya}\, e^{j\beta\hat{r}.\underline{r}'} da$$

$$= \int_{-a/2}^{a/2}\int_{-b/2}^{b/2} E_{ya} e^{j\beta(x\cos\theta_1\cos\varnothing_1 + y\sin\theta_1\sin\varnothing_1)} dydx \text{.... (3)}$$

$$\boldsymbol{\beta} = \boldsymbol{\varpi}\sqrt{\boldsymbol{\mu}_0\boldsymbol{\varepsilon}_0}\ ,\ Z_0\ \sqrt{\boldsymbol{\mu}_0 / \boldsymbol{\varepsilon}_0}\ ,\ \text{thus } \boldsymbol{\beta} / Z_0 = \boldsymbol{\omega\varepsilon}$$

The boundary conditions on the surface of the sub-reflector require that the tangential components of the electric field to be zero whereas the tangential components of the magnetic field are doubled. Expressing $\hat{\theta}$ and $\hat{\varnothing}$ in rectangular coordinate system and retaining only the x-and y-components, the tangential magnetic field on the surface of the sub-reflector is then given by:

$$\underline{H}_{ts} = -j\boldsymbol{\omega\varepsilon}\frac{e^{-j\beta r_1}}{2\pi r_1}(1+\cos\boldsymbol{\theta}_1)P_y[\hat{x}(\cos\boldsymbol{\theta}_1\cos^2\varnothing_s + \sin^2\varnothing_s)$$

$$+\hat{y}(1-\cos\boldsymbol{\theta}_1)\sin\varnothing_s\cos\varnothing_s] = \hat{x}H_{xs} + \hat{y}H_{ys} \text{ ....(4)}$$

where $\varnothing_s = \pi - \varnothing_1$.

The radiation fields set up at an observation point P(r_2, θ_2, $\varnothing_2$) due to the electric surface current density, which is associated with $\underline{H}_{ts}$ are:

$$\underline{E}_2 = j\omega\boldsymbol{\mu}\frac{e^{-j\beta r_2}}{2\pi r_2}\Big[\hat{\theta}\cos\theta_2(Q_{xs}\sin\varnothing_2 - Q_{ys}\cos\varnothing_2)$$

$$+ \hat{\varnothing}(Q_{xs}\cos\varnothing_2 + Q_{ys}\sin\varnothing_2\Big] \text{.....(5-a)}$$

$$\underline{H}_2 = \frac{1}{Z_0}\hat{r}\times\underline{E}_2 = -j\beta\frac{e^{-j\beta r_2}}{2\pi r_2}\Big[\hat{\theta}(Q_{xs}\cos\varnothing_2 + Q_{ys}\sin\varnothing_2$$

$$-\hat{\varnothing}\cos\theta_2(Q_{xs}\sin\varnothing_2 - Q_{ys}\cos\varnothing_2)\Big] \text{....(5-b)}$$

The functions Q_{xs} and Q_{ys} are defined by:

$$Q_{xs} = \int_s \underline{H}_{xs}\, e^{j\beta\hat{r}.\underline{r}'} da \text{ ....(6-a)}$$

$$Q_{ys} = \int_s \underline{H}_{ys}\, e^{-j\beta\hat{r}.\underline{r}'} da \text{ ....(6-b)}$$

where the integration is now over the cross-section area of the sub-reflector which lies in the xy-plane, so $da = \hat{\rho}_s\, d\rho_s d\varnothing_s$ and $\underline{r}' = \hat{\rho}_s\rho_s$. This with $\hat{r} = \hat{\rho}_s \sin\theta_2 \cos(\varnothing_2 - \varnothing_s) + \hat{z}\cos\varnothing_s$ yields

$\hat{r}.\underline{r}' = \hat{\rho}_s \sin\theta_2 \cos(\varnothing_2 - \varnothing_s)$ and hence

$$Q_{xs} = \int_0^{2\pi}\int_0^{r} H_{xs} e^{j\beta\rho_s\sin\theta_2\cos(\varnothing_2 - \varnothing_s)}\rho_s d\rho_s d\varnothing_s \text{ ....(7-a)}$$

$$Q_{ys} = \int_0^{2\pi}\int_0^{r} H_{ys} e^{j\beta\rho_s\sin\theta_2\cos(\varnothing_2 - \varnothing_s)}\rho_s d\rho_s d\varnothing_s \text{ ....(7-b)}$$

Again, the boundary conditions imposed by a perfect conductor of the main-reflector lead to:

$$H_{tm} = -j\boldsymbol{\beta}\frac{e^{-j\beta r_2}}{2\pi r_2}\cos\boldsymbol{\theta}_2(\hat{x}Q_{xs} + \hat{y}Q_{ys}) \text{ ....(8)}$$

The radiation electric field set up at an observation point P(r_3, θ_3, $\varnothing_3$) in the far-field region due to the electric surface current density, which is associated with $\underline{H}_{tm}$, on the main-reflector, is

$$\underline{E}_3 = -j\boldsymbol{\omega\mu}\frac{e^{-j\beta r_3}}{2\pi r_3}\Big[\hat{\boldsymbol{\theta}}\cos\boldsymbol{\theta}_3(Q_{xm}\sin\varnothing_3 - Q_{ym}\cos\varnothing_3)$$

$$+ \hat{\varnothing}(Q_{xm}\cos\varnothing_3 + Q_{ym}\sin\varnothing_3\Big] \text{ ....(9)}$$

where

$$Q_{xm}=\int_s H_{xm}e^{j\beta\hat{r}\cdot r'}da$$

$$=\int_0^{2\pi}\int_0^{r} H_{xm}e^{j\beta\rho_m\sin\theta_3\cos(\varnothing_3-\varnothing_m)}\rho_m d\rho_m d\varnothing_m \ldots (10\text{-a})$$

$$Q_{ym}=\int_s H_{ym}e^{j\beta r\cdot r'}da$$

$$=\int_0^{2\pi}\int_0^{r} H_{ym}e^{j\beta\rho_m\sin\theta_3\cos(\varnothing_3-\varnothing_m)}\rho_m d\rho_m d\varnothing_m \ldots (10\text{-b})$$

It is evident that $\varnothing_m=\pi-\varnothing_2$ and the integration above is taken over the cross-section area of the main-reflector.

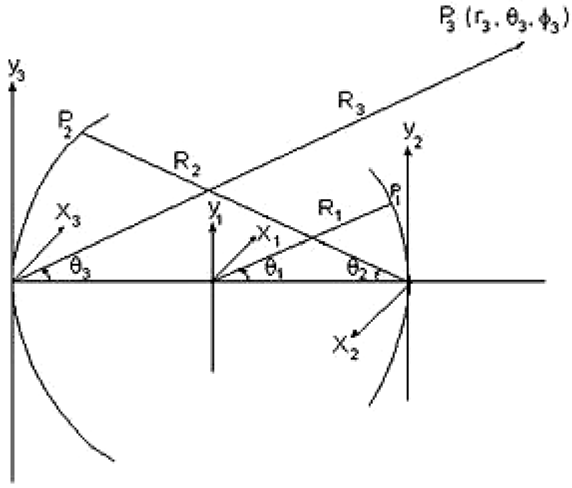

Figure 2: SBFA and coordinate system.

RESULTS

The radiation field pattern in the principle E-and-H-planes are obtained from (formula 9) by numerically evaluating the appropriate integrals. These patterns are compared in Figures 3 and 4, respectively with the corresponding experimental results of Large (6) and Leong (8). Two sets of theoretical patterns are indicated in each figure. In the first one the physical and virtual radii are equal, whereas in the other one the virtual radius is slightly larger than the physical. A good agreement between the theoretical and experimental patterns is noted for the main lobe, and nearly identical half power beam-widths, are obtained in both figures. Some deviation in the side lobe level specially in the E-plane pattern may be attributed to the experimental errors and the negligible radiation difracted from the edge of the subreflector in the calculated pattern.

It is to be emphasized that there is some area on the surface of the main reflector occupied by the feeder. It is for that reason the integration over the radius of the main reflector in (formula 10) is taken

Figure 3: Radiation field patterns in E and H-planes of short backfire antenna.

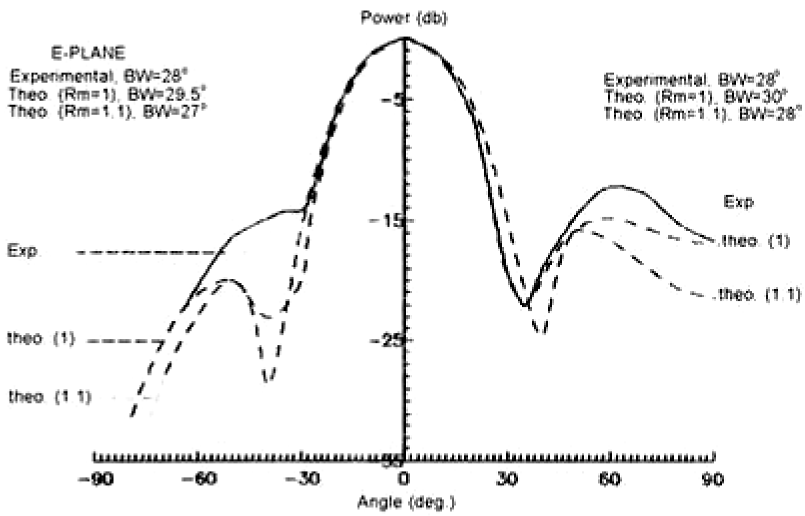

from 0.286l instead of the origin. This value corresponds to the radius of the equivalent area blocked by the feeder.

Finally, it should be mentioned that the results discussed above are obtained with no effort made to consider the effect of the edge diffraction and/or near-zone field measurement. These two parameters are still to be investigated. However, it was found that the edge diffraction could be significantly reduced by providing a small rim around the edge of the main reflector (2). The near-field contribution which has been overlooked in this analysis may be overcome by taking the virtual radius of the main reflector slightly larger than the physical one (12) as mentioned above and gives even better agreement between analytical and experimental patterns.

CONCLUSION

It is concluded that the radiation fields of a short backfire antenna may be mathematically formulated in a close form by using the current distribution method. This analytical technique provides a greater insight into the basic nature of the short backfire antenna.

REFERENCES

1. Ehrenspeck HW : The backfire antenna, a new type of directional line source Proc IRE (correspondence). Vol 48, pp 109-110, 1960.

2. Ehrenspeck HW : The short backfire antenna Proc IEEE (correspondence), pp 1138-1140, 1965.

3. Ehrenspeck HW : The backfire antenna, new results, Proc IEEE (correspondence). Vol 53, pp 639-641, 1965.

4. Long MS and PS Kook : Rectangular wave guide excited short backfire antenna with corrugated rim. Electronics Letters, pp 533-535, 1970.

5. Potel DC : Directivity of the short backfire antenna. Vol 118, Proc IEEE, pp 1550-1552, 1971.

6. Large AC : Short backfire antenna with waveguide and linear fields. Microwave Journal, vol 19, pp 49-52, 1975.

7. Ohmori S, S Miura, K Kameyama and H Yoshimura : An improvement in electrical characteristics of a short backfire antenna, IEEE Transactions on Antennas and Propagation. Vol Ap-31, pp 644-646, 1983.

8. Leong MS and PS Kooi : Performance of a rectangular waveguide excited short backfire antenna employing a conical main reflector. Electronics Letters, vol 20, pp 749-751,1984.

9. Al-Rashid R, S Marougi and Z Ahmed : Short backfire antenna with circular waveguide feed and conical back reflector. 21st international electronics conference and exhibition IRE, Australia, pp 305-307, 1987.

Figure 4: Radiation field patterns in E and H-planes of short backfire antenna.

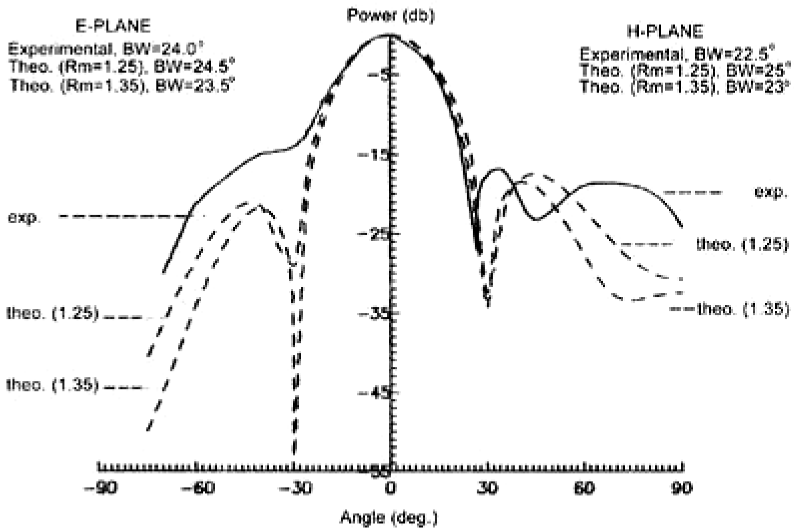

10. Al-Rashid R, MM El-Kadi : Short backfire antenna with double flat back reflector and rectangular aperture as feed element. Journal of Islamic Academy of Science. Vol 6, pp 3-7, 1993.

11. Zuker PJ : The backfire antenna; Aqualitative approach to its design. Proc IEEE, vol 53, pp 746-747, 1965.

12. Chen KM, DP Nyquist and JL Lin : Radiation fields the short backfire antenna. IEEE Transaction on Antenna and Propagation, vol UP-16, pp 596-597, 1968.

13. Loh SC and WS Leunge : The radiation field of the short backfire antenna. The radio and electronic engineer, vol 39, pp 198-200, 1970.

14. Stutzman WL and GA Thiele : Antenna theory and design. John Wiley and Sons, New York, pp 380-383, 1981.

Correspondence:
Z. A. Ahmed
Department of Physics,
College of Science,
University of Basrah,
Basrah, IRAQ.